cells

MDPI

Article

Changes in Mitochondrial Size and Morphology in the RPE and Photoreceptors of the Developing and Ageing Zebrafish

Thomas Burgoyne [1,2,†], Maria Toms [1,3,†], Chris Way [1], Dhani Tracey-White [1], Clare E. Futter [1] and Mariya Moosajee [1,3,4,5,*]

1 UCL Institute of Ophthalmology, University College London, London EC1V 9EL, UK
2 Royal Brompton Hospital, Guy's and St Thomas' NHS Foundation Trust, London SW3 6NP, UK
3 The Francis Crick Institute, London NW1 1AT, UK
4 Department of Ophthalmology, Great Ormond Street Hospital for Children NHS Foundation Trust, London WC1N 3JH, UK
5 Department of Genetics, Moorfields Eye Hospital NHS Foundation Trust, London EC1V 2PD, UK
* Correspondence: m.moosajee@ucl.ac.uk
† These authors contributed equally to this work.

Abstract: Mitochondria are essential adenosine triphosphate (ATP)-generating cellular organelles. In the retina, they are highly numerous in the photoreceptors and retinal pigment epithelium (RPE) due to their high energetic requirements. Fission and fusion of the mitochondria within these cells allow them to adapt to changing demands over the lifespan of the organism. Using transmission electron microscopy, we examined the mitochondrial ultrastructure of zebrafish photoreceptors and RPE from 5 days post fertilisation (dpf) through to late adulthood (3 years). Notably, mitochondria in the youngest animals were large and irregular shaped with a loose cristae architecture, but by 8 dpf they had reduced in size and expanded in number with more defined cristae. Investigation of temporal gene expression of several mitochondrial-related markers indicated fission as the dominant mechanism contributing to the changes observed over time. This is likely to be due to continued mitochondrial stress resulting from the oxidative environment of the retina and prolonged light exposure. We have characterised retinal mitochondrial ageing in a key vertebrate model organism, that provides a basis for future studies of retinal diseases that are linked to mitochondrial dysfunction.

Keywords: mitochondria; ageing; retina; zebrafish

Citation: Burgoyne, T.; Toms, M.; Way, C.; Tracey-White, D.; Futter, C.E.; Moosajee, M. Changes in Mitochondrial Size and Morphology in the RPE and Photoreceptors of the Developing and Ageing Zebrafish. *Cells* **2022**, *11*, 3542. https://doi.org/10.3390/cells11223542

Academic Editors: Yuguang Shi and Jun Zhang

Received: 11 August 2022
Accepted: 4 November 2022
Published: 9 November 2022

1. Introduction

Mitochondria are essential intracellular organelles that provide energy for cells in the form of adenosine triphosphate (ATP), generated through oxidative phosphorylation [1,2]. In addition, they perform a variety of crucial cellular functions including regulating apoptosis, scavenging reactive oxygen species (ROS), calcium homeostasis, nucleotide metabolism, and the biosynthesis of amino acids, cholesterol and phospholipids. Mitochondrial populations are dynamic, showing alterations throughout the lifespan of an organism resulting from fission (division of a mitochondrion into two daughter mitochondria), fusion (merging of two mitochondria into one larger mitochondrion) and mitophagy (selective removal of dysfunctional mitochondria) [3]. These processes allow them to maintain cellular homeostasis and meet the energy requirements of the tissue but are also associated with ageing and disease when defective. Examples of retinal disease resulting from defective mitochondria include Kearns Sayre syndrome, neuropathy, ataxia and retinitis pigmentosa (NARP), and mitochondrial encephalomyopathy, lactic acidosis and stroke-like episodes (MELAS) [4].

Although the diverse functions of mitochondria make them critical for all cell types, mitochondrial populations are most dense in energy intensive tissues like the retina [2,5]. The photoreceptors consume more oxygen per gram of tissue weight than any other cell type and their inner segment ellipsoids contain numerous mitochondria necessary

for high levels of ATP production [5,6]. Among the mitochondria of the photoreceptor ellipsoid, significantly larger organelles, sometimes referred to as 'megamitochondria', have been noted in certain species such as shrews [7,8] and some teleost species including zebrafish [9,10]. During development, these large mitochondria have been proposed to form from the enlargement of individual mitochondria [11]. As the retinal pigment epithelium (RPE) is essential for nourishing the photoreceptors and supporting their high metabolic activity, abundant mitochondria also populate this tissue [1,12].

Due to a number of factors, including ROS accumulation caused by elevated ATP generation and light exposure, the mitochondria of the RPE and photoreceptors are particularly vulnerable to dysfunction over time [13,14]. Alterations in the number and morphology of mitochondria, related to an impaired balance of mitochondrial dynamics, have been observed in ageing retinal tissue and are associated with ocular diseases such as age-related macular degeneration and Leber congenital amaurosis [1,12,15]. Some of these changes can be attributed to mitochondrial fission or fusion. These two processes involve discrete sets of proteins that localise to mitochondria to perform specialised roles. During mitochondrial fusion, Mitofusins Mfn1 and Mfn2 aid the tethering of mitochondria to each other and Opa1 alters the biophysical properties of the lipids in the mitochondrial inner membrane [16]. When fission occurs, Fis1 has been proposed to interact with Drp1 to form a collar around the mitochondria that acts to separate them [17].

Previously, age-related changes in the retinal mitochondria have been described in several species, including human [18,19], macaque [20], and mouse [6]. The zebrafish is a popular model for ocular studies and the ultrastructure of the larval zebrafish photoreceptors and adult retina has been characterised [21,22]. However, there has been limited examination of mitochondrial changes throughout the lifespan of the zebrafish retina. In the present study, we have performed ultrastructural analysis to investigate both the development and ageing of mitochondria in the zebrafish RPE and photoreceptors, providing an alternative vertebrate model of retinal ageing.

2. Materials and Methods

2.1. Zebrafish Husbandry

Zebrafish (wild-type, AB strain) were bred and maintained according to local UCL and UK Home Office regulations for the care and use of laboratory animals under the Animals Scientific Procedures Act, at the UCL Institute of Ophthalmology animal facility. Zebrafish were raised at 28.5 °C on a 14 h light/10 h dark cycle. UCL Animal Welfare and Ethical Review Body approved all procedures for experimental protocols, in addition to the UK Home Office (License no. PPL PC916FDE7). All approved standard protocols followed the guidelines of the Association for Research in Vision and Ophthalmology (ARVO) Statement for the Use of Animals in Ophthalmic and Vision Research Ethics [23]. All zebrafish were euthanised for enucleation at the same time of day in the afternoon.

2.2. Mice

Eyes were acquired from mice that had been killed by cervical dislocation in accordance with Home Office (United Kingdom) guidance rules under project license 70/8401. This was done adhering to the ARVO Statement for the Use of Animals in Ophthalmic and Vision Research.

2.3. Transmission Electron Microscopy

At given timepoints, zebrafish were terminally anaesthetized in 0.2 mg/mL Tricaine (MS-222) and the eyes were harvested through enucleation if 1 mpf or older. Enucleated zebrafish eyes or whole larvae were fixed in 2% paraformaldehyde/2% glutaraldehyde in 0.15 M cacodylate buffer prior to incubation with 1% osmium tetroxide/1% potassium ferrocyanide. Following dehydration in an ethanol series and propylene oxide, the zebrafish were embedded in EPON resin. Using a Leica EM UC7 ultramicrotome, 100 nm sections were cut, collected on copper grids (EMS) and stained with lead citrate. Sections were

examined on a JEOL 1010 and JEOL 1400Plus TEM, both equipped with a Gatan Orius SC1000B charge-coupled device camera. Images were analysed using the ImageJ software.

2.4. RT-qPCR

Total RNA was extracted from enucleated zebrafish eyes using the RNeasy micro kit (Qiagen, UK) according to the manufacturer's instructions. Using 1 µg total RNA, cDNA was reverse transcribed using the Superscript III First-strand synthesis Supermix kit (Thermo Fisher). For quantitative real-time PCR amplifications, gene expression was quantified using SYBR Select fluorescent dye (Thermo Fisher) in triplicate reactions for each sample. All RT-qPCR primers are listed in Table 1. The expression of each gene was normalized to the housekeeping gene *β-actin*. The StepOne Plus RealTime PCR System (Thermo Fisher) was used and reactions analysed using the Comparative CT experiment option in the StepOne software (Version 2.3).

Table 1. RT-qPCR primers used in this study.

Gene	Forward Primer (5′-3′)	Reverse Primer (5′-3′)
polg2	GTGGAGGAAGTTTGCTTTAGGCCCG	GGGTCCACAGTGTCTCCAGCGT
opa1	GCCGGAAGTGTAGTTACCTG	AGGTGGTCTCTGTGGGTTGT
mfn1	CTGGGTCCCGTCAACGCCAA	ACTGAACCACCGCTGGGGCT
fis1	ACAGACTTAAGGAGTATGAGAGAGC	AATACCACCGACAATCGCCA
pink1	AACACTACCCTTGAAGAATG	AAATCTGAAGGCTTTTACGG
sod2	ACAGCAAGCACCATGCAACA	CAGCTCACCCTGTGGTTCTCC
β-actin	TGTACCCTGGCATTGCTGAC	TGGAAGGTGGACAGGGAGGC

2.5. RNAscope Assay

Whole zebrafish larvae (5 and 8 dpf) or enucleated zebrafish eyes (1 mpf and 12 mpf) were fixed in 4% PFA/PBS at 4 °C overnight. After washing three times in PBS for 10 min, the eyes/larvae were incubated in 10, 20 and 30% sucrose/PBS at 4 °C overnight each time. The samples were embedded in Tissue-Tek O.C.T embedding medium (VWR) using dry ice and 12 µm cryosections were collected onto Superfrost PLUS slides (Fisher Scientific) using a Leica CM3050S cryostat. The RNAscope assay was performed on cryosections using the RNAscope Fluorescent Multiplex kit (ACD). The *fis1* and *opa1* probes were designed and provided by ACD. Images were taken on a Zeiss Upright 710 confocal microscope.

2.6. Statistics

Data are shown as mean values ± standard deviation from n observations. Student's t-tests, Mann–Whitney test or one way-ANOVA were used to compare data. $p < 0.05$ was accepted to indicate statistical significance (*).

3. Results

3.1. Alterations in the Mitochondrial Morphology within Zebrafish Retina during Development and Ageing

3.1.1. Retinal Pigment Epithelium (RPE)

Mitochondria within the RPE were examined in zebrafish from 5 days post fertilisation (dpf) up to 36 months post fertilisation (mpf) by transmission electron microscopy (TEM) (Figure 1). In the RPE, a large number of mitochondria were concentrated at the basal surface adjacent to Bruch's membrane. The RPE of 5 and 8 dpf fish contained a small number of notably large mitochondria. This includes some mitochondria that had an area exceeding 0.8 μm^2 that was not found at other time points (see further examples at 5 dpf in Figure S1). By 1 mpf, a dramatic decrease in size and increase in mitochondrial number was observed. With age, the mitochondria continued to increase in number with a

modest decrease in size. Morphologically the mitochondria had a similar appearance at all timepoints except 5 and 8 dpf, where they had a more irregular shape and the cristae architecture appeared less well defined.

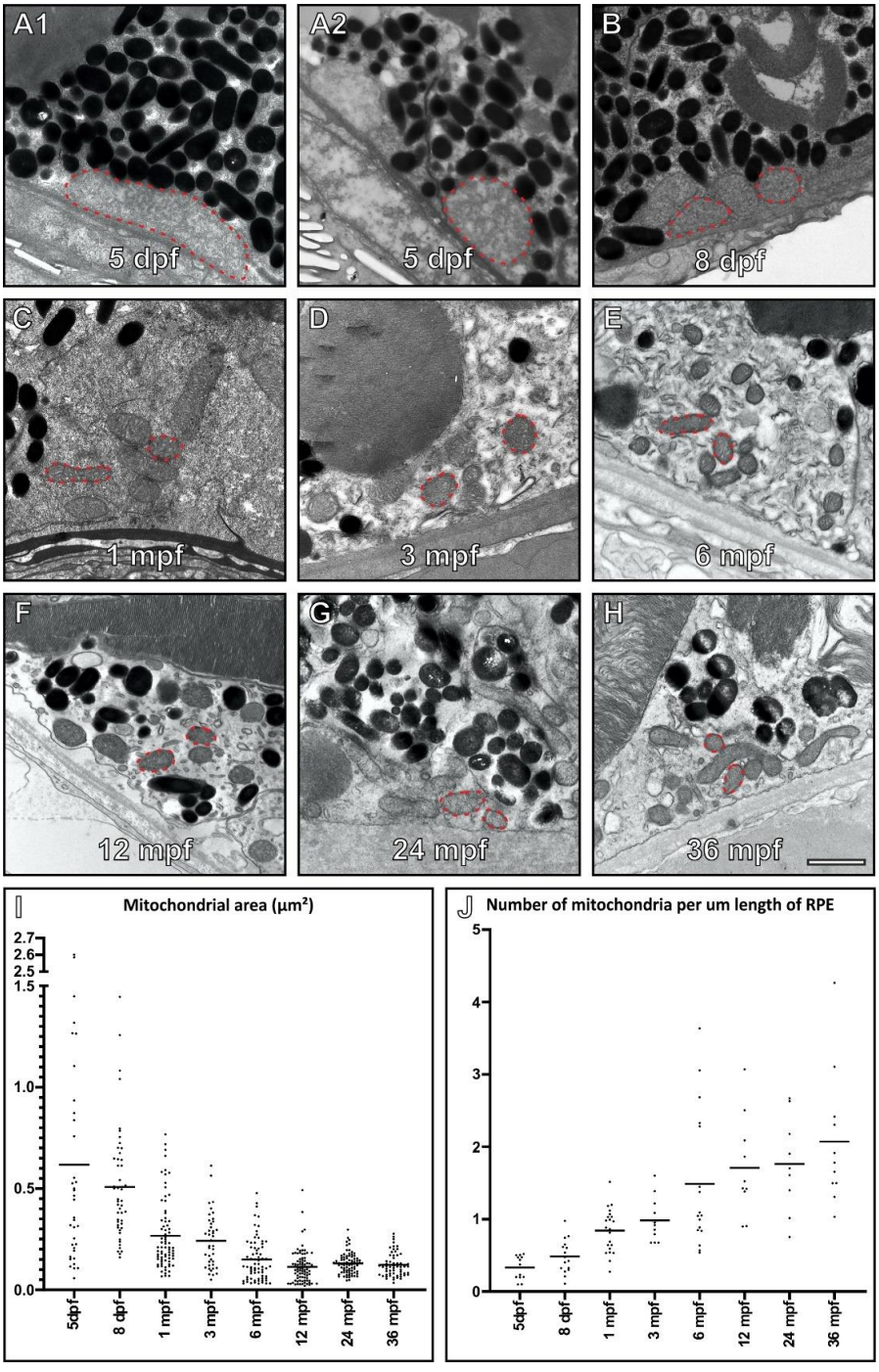

Figure 1. Mitochondria increase in number and decrease in size within the retinal pigment epithelium (RPE) of ageing zebrafish retina. (**A**–**H**) Electron microscopy images of mitochondria within zebrafish RPE at 5 dpf through to 36 mpf. The red dotted lines indicate examples of mitochondria within the RPE at each timepoint. All mitochondria were measured in random areas of RPE. When individual mitochondria are examined within the RPE, they (**I**) decrease in size and (**J**) increase in number as the zebrafish age. (**I**,**J**) At each timepoint, n = 3 zebrafish were examined, and measurements taken from (**I**) $\geq$ 34 mitochondria per age group and (**J**) $\geq$ 8 regions of the RPE. Statistical significance determined by one way-ANOVA (**I**–**J**) with $p < 0.0001$. Scale (**A**–**G**) 1 µm.

3.1.2. Photoreceptor Inner Segments

We examined the morphology of mitochondria within zebrafish rod photoreceptor inner segments (ISs) with age. Rods could be readily distinguished from cones by their proximity to the inner retina and their inner and outer segment shape [24]. Mitochondria were examined from 5 dpf up to 36 mpf by TEM (Figure 2). At 5 dpf, the rod photoreceptors contained large mitochondria within their ISs bundled together in a spherical arrangement, similar to the observations described in a previous study [22]. By 8 dpf, there was a small decrease in size, accompanied by the appearance of more well-defined cristae, reflecting what was observed within the RPE. With age, mitochondrial number continued to increase at least up until 12 months with a small decrease in size; the morphology of the mitochondria did not appear to alter dramatically.

Cone photoreceptor IS mitochondria were compared at 5 dpf and 1 mpf to determine if a similar change in mitochondrial morphology occurred as observed in the rods (Figure 3). At 5 dpf the retina is still developing, and it is difficult to distinguish different cone subtypes unlike at 1 mpf. Therefore, we focused on the UV cones due to them being identifiable, as they are positioned furthest away from the RPE cell layer (see Figure S2). The morphology of the mitochondria in 5 dpf UV cone ISs was clearly different to the UV cones identifiable at 1 mpf. At 5 dpf, the mitochondria appeared to be packed together in a spherical like arrangement. In the fully developed retina at 1 mpf, the mitochondria were still bundled together but more numerous and arranged according to size, with larger mitochondria located more adjacent to the outer segment in the red and green cones, as previously described [21,22]. At 5 dpf and 1 mpf the mitochondrial membranes of neighbouring mitochondria in UV cones appeared closely associated.

Comparison of the mitochondrial morphology in rods (Figure 2) and cones (Figure 3) suggested that the cristae of rod mitochondria were more tightly packed than those of UV cones. To assess the structure of rod and UV cone IS mitochondria at 5 dpf in detail, tomograms were generated (Figure 4 and Videos S1 and S2). These provide higher-resolution data than conventional TEM, in the form of reconstructions that allow mitochondrial membranes to be visualised in 3D. The outer mitochondrial membranes of neighboring mitochondria were seen to be in close proximity with a uniform spacing between them of 7.66 nm ($\pm$1.43) and 7.67 nm ($\pm$1.63) for rods and UV cones, respectively. Consistent with our observations on multiple cells in Figure 2, Figures 3 and S2 the rod IS mitochondria clearly had more tightly packed sheet-like cristae than those of mitochondria within UV cones.

3.2. Morphology of Mitochondria within the Retina of Embryonic and Adult Mice

To investigate if a notable change in mitochondrial size is seen in the retina of other organisms during retinal development, RPE and photoreceptors of embryonic day 14 (E14), postnatal day 13 (P13) and 6-month-old adult mice were examined (Figure 5). At E14, the photoreceptor outer segments (OSs) had not yet formed and the ISs were positioned up against the RPE layer (Figure 5A–C). As zebrafish develop more rapidly than mice, the rate of mitochondria maturation in the retina most likely differs. The first signs of eye development in mice are detected around E8 and in zebrafish 16 hours post fertilisation [25,26]. Therefore, the E14 mice examined represent an early timepoint in eye development, where retinal mitochondrial maturation is still ongoing. P13 mouse retina was more similar in appearance to the 5 dpf zebrafish time-point, as the outer segments are almost fully formed in both (Figures 3A,B and 5D,E). Zebrafish have been reported to have visual function from 3 dpf whereas mice open their eyes at around P11 [26,27]. Therefore, it can be predicted that both 5 dpf zebrafish and P13 mice will have been visually active for ~48 h. When examining the mitochondria within the RPE, there was little difference in their size when comparing the E14, P13 and adult mouse retina (Figure 5B,E,H). There was a greater difference in the IS mitochondria—at E14 they were shorter in length than at P13 and in adults (Figure 5C,F,I). Notably, the mitochondria in the adult mouse IS are more elongated that in zebrafish, less packed and most are in contact with the plasma membrane.

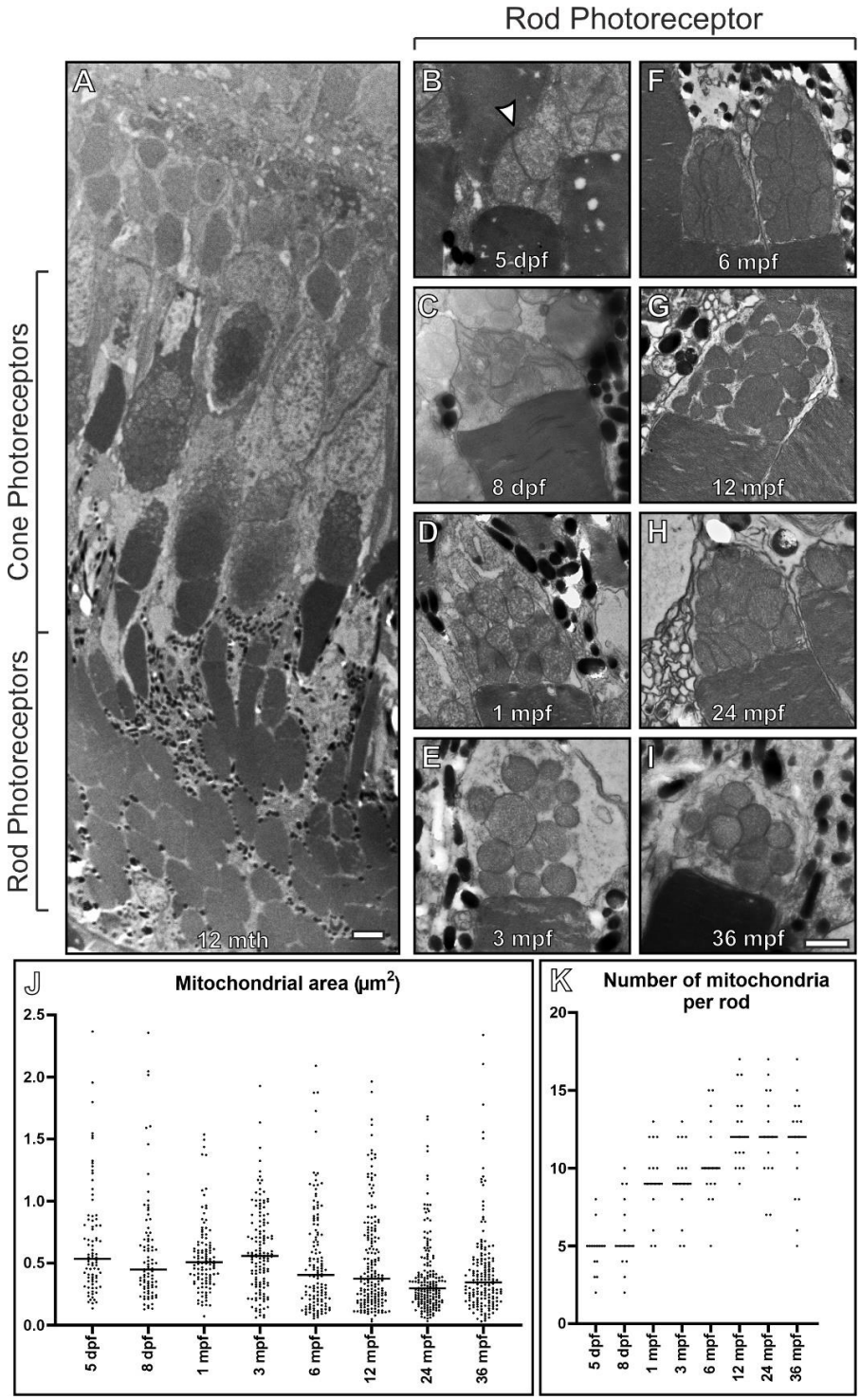

Figure 2. Rod inner segments of early embryonic zebrafish have compact mitochondria with a morphology different from other ages. (**A**) Electron microscopy image of 12 mpf retina between the RPE and ONL that includes rod and cone photoreceptor outer (POS) and inner segments. (**B**–**I**) Images of rod photoreceptor inner segments at 5 dpf through to 36 mpf. (**B**) At 5 dpf, the mitochondria are bundled together in a spherical like arrangement and there is a morphology change by (**C**) 8 dpf, with further changes by (**D**) 1 mpf as the mitochondria become less clumped together. There is (**J**) a reduction in rod inner segment mitochondrial size and (**K**) an increase in mitochondria number with time. Measurements were acquired from n = 3 zebrafish and included (**J**) >83 mitochondria and (**K**) n = 15 rods at each timepoint. (**J**,**K**) Statistical significance determined by one way-ANOVA (**J**,**K**) with $p < 0.0001$. Scale (**A**) 10 μm, (**B**–**I**) 1 μm.

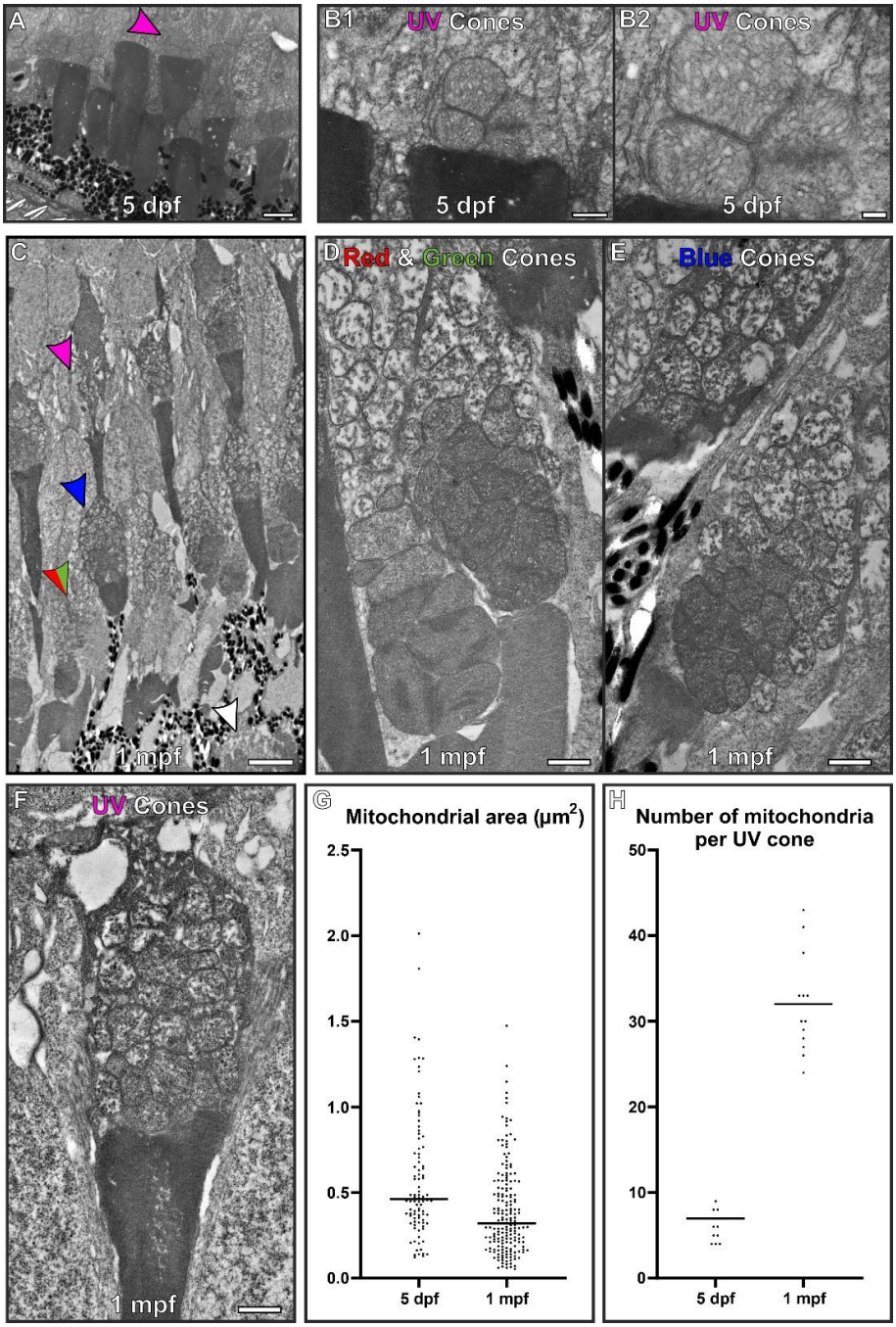

Figure 3. At 5 dpf, the mitochondria within cone inner segments have a morphology that is distinct from those found within 1 month old zebrafish. (**A**) At 5 dpf, the retina is still developing and it is difficult to distinguish between cone types. UV cones (purple arrowhead) were identifiable due to being positioned furthest from the RPE cell layer. (**B**) Higher magnification images of UV cone containing packed mitochondria. (**C**) By 1 mpf, the retina has fully formed and the different photoreceptors can be readily identified. The arrows highlight the inner segment from different photoreceptors: red and green arrows for red and green cones, blue arrows for blue cones, purple arrows for the UV cones and white arrowz for rod photoreceptors. (**D**–**F**) The corresponding cone types at 1 mpf are shown at higher magnification. (**G**) Mitochondria were found to reduce in size and (**H**) increase in number from 5 dpf to 1 mpf. Measurements were taken from n = 3 zebrafish and included (**G**) >93 mitochondria and (**H**) n = 15 UV cones. Statistical significance was determined as (**G**) $p < 0.001$ by Mann–Whitney test (non-parametric based on Kolmogorov–Smirnov test) and (**H**) $p < 0.001$ by unpaired *t*-test. Scale (**A**,**C**) 5 μm, (**B**,**D**–**F**) 1 μm.

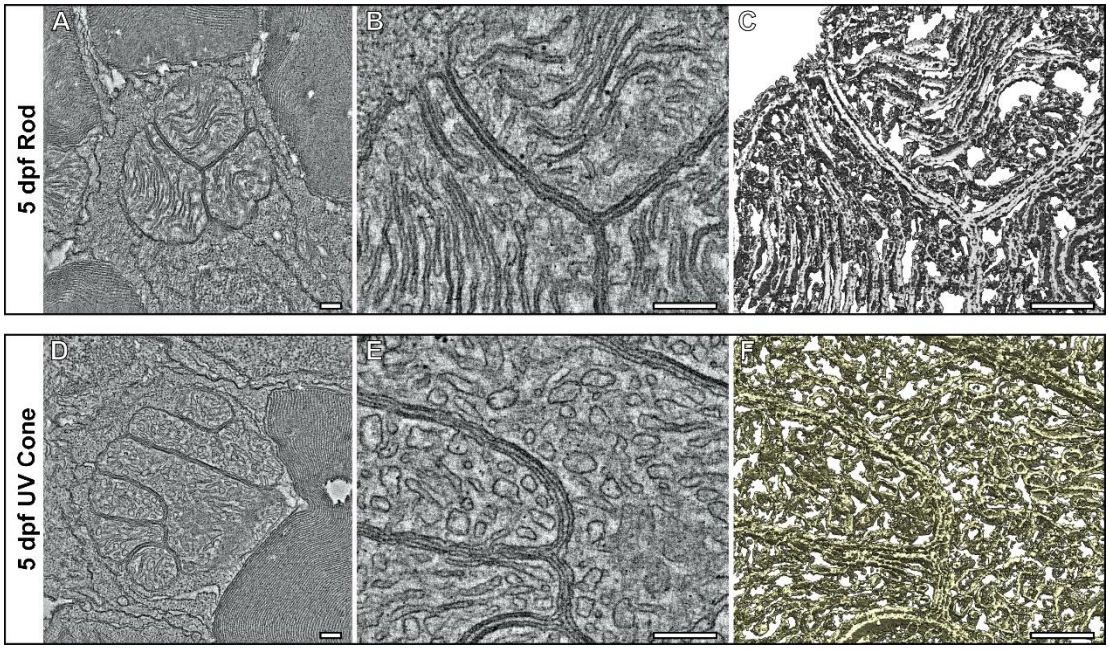

Figure 4. Tomograms show the compact association of mitochondria within the inner segments of UV cone and rod photoreceptors at 5 dpf. (**A**–**C**) Tomography data of rod and (**D**,**E**) UV cone inner segment mitochondria. (**A**,**D**) Single slices from the tomograms with (**B**,**E**) higher magnification views. (**C**–**F**) Surface rendering of the tomography data allows the architecture of the mitochondria to be assessed in 3D. The rod has elongated and tightly associated cristae membranes, whereas the UV cone has cristae that are wider. Scale bars = 250 nm.

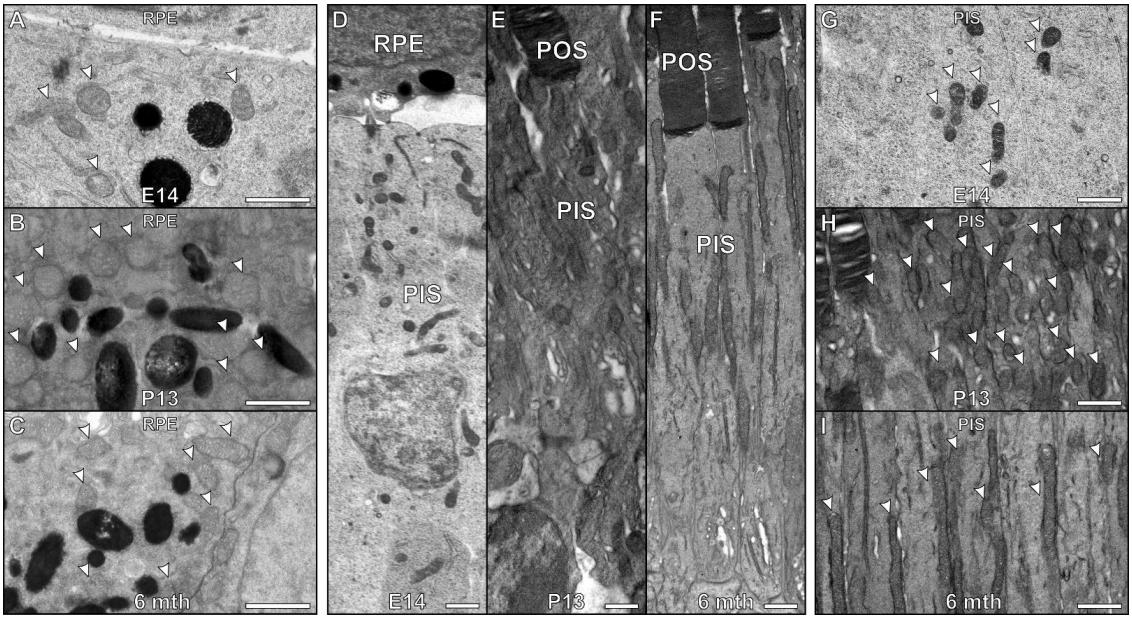

Figure 5. Age-related changes in mitochondrial size in zebrafish are not replicated in developing mouse retinas. (**A**–**C**) There is little difference between the mitochondria within the RPE at (**A**) embryonic day 14 (E14) compared to a (**B**) postnatal day 13 (P13) and (**C**) 6 month old mouse (**D**–**F**) By E14, mouse retina is still developing and photoreceptors do not have fully formed outer segments (POS). At P13, the mouse has photoreceptors with almost fully developed POS. (**G**–**I**) There is a clear difference in the photoreceptor inner segment mitochondria. (**G**) The mitochondria are smaller at E14 compared to (**H**) P13 and (**I**) 6 month old mouse. At P13, the appearance of the (**B**) RPE and (**E**,**H**) photoreceptors are similar to (**C**,**F**,**I**) at 6 months in adult mice. Scale bars (**A**–**I**) 1 µm.

3.3. Age-Related Changes in Mitochondria-Associated Genes

To examine factors regulating mitochondrial size and number in the zebrafish retina, RT-qPCR analysis was performed to assess the gene expression of several indicators of mitochondrial activity: *polg2* (mitochondrial DNA replication), *fis1* (fission), *opa1* (fusion), *mfn1* (fusion), *pink1* (mitophagy) and *sod2* (antioxidant enzyme) (Figures 6 and 7). To explore how expression levels change with age, all genes were analysed at 5 dpf, 1 mpf, 12 mpf and 24 mpf. *polg2* showed increased expression at 1 mpf relative to 5 dpf (6.8 ± 1.47 fold; $p < 0.0001$, n = 5) (Figure 6A). This increased expression was also present at 12 mpf, (6.5 ±1.26 fold, $p < 0.0001$, n = 5). At 24 mpf, expression of *polg2* was 4.8 ±2.23 fold higher than that at 12 mpf, but this difference was not significant ($p = 0.08$) (Figure 6B).

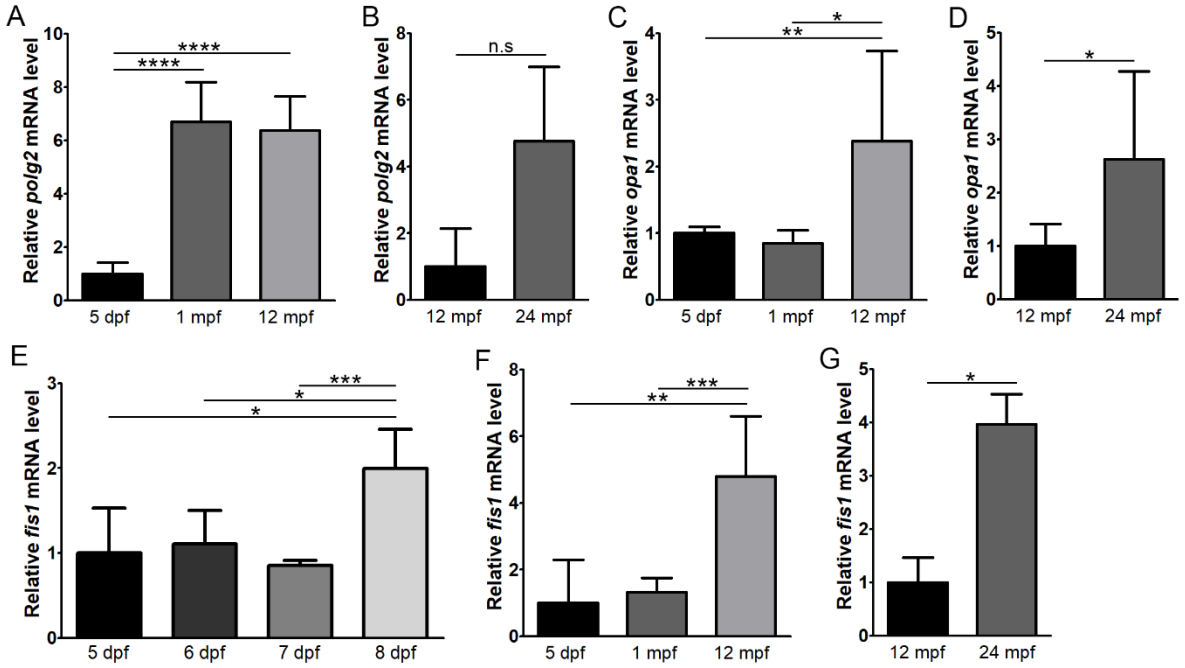

Figure 6. Expression levels of *polg2*, *opa1* and *fis1* with age in the zebrafish retina. RT-qPCR was performed to assess expression of *polg2* (**A**,**B**), *opa1* (**C**,**D**) and *fis1* (**E**–**G**) at 5 days post-fertilisation (dpf), 1 month post-fertilisation (mpf), 12 mpf and 24 mpf (n = 5). Expression of *fis1* was also assessed at 5–8 dpf (n = 4) (**E**). * $p < 0.05$; ** $p < 0.01$; *** $p < 0.001$; **** $p < 0.0001$; n.s, not significant.

Reduced mitochondrial fusion could lead to the increased mitochondrial numbers and reduced size that was observed with age. However, both markers of fusion, *opa1* and *mfn1*, maintained similar expression levels between the 5 dpf and 1 mpf timepoints (Figure 6C and Supplementary Figure S3). *opa1* expression increased to 2.4 ± 1.35 at 12 mpf, which was significantly upregulated compared to both earlier timepoints ($p < 0.01$). At 24 mpf, *opa1* expression also significantly increased by 2.6 ± 1.65 fold compared to 12 mpf ($p < 0.05$). *mfn1* was upregulated at 12 mpf by 6.8 ± 4.17 fold ($p < 0.01$) and 24 mpf by 3.7 ± 2.31 fold, but not quite significantly at the latter ($p = 0.06$). To further investigate expression of *opa1* during development and ageing, we performed an RNAscope assay on zebrafish retinas at 5 dpf, 8 dpf, 1 mpf and 12 mpf (Supplementary Figure S4). *opa1* transcripts showed an increase at 12 mpf in both the photoreceptors and RPE.

Enhanced mitochondrial fission could also lead to increased mitochondrial numbers and reduced size. At 1 mpf, expression of *fis1* was not significantly different compared to 5 dpf, showing 1.3 ± 0.42 fold relative expression (n = 5) (Figure 6F). However, given the substantial increase in mitochondrial numbers that were seen within only 3 days between 5 and 8 dpf (Figure 1), we explored *fis1* expression during this time period. Although it was relatively unchanged at 5–7 dpf, there was a 2.0 ± 0.46 fold increase at 8 dpf relative to 5 dpf ($p < 0.05$, n = 4) (Figure 6E). At 12 mpf, *fis1* expression was upregulated by 4.8 ±1.80

fold compared to 5 dpf ($p < 0.01$), which was also significantly higher than expression at 1 mpf ($p < 0.001$) (Figure 6F). In addition, expression at 24 mpf (n = 4) was 4.0 ± 0.57 fold greater than 12 mpf ($p < 0.05$) (Figure 6G). Examination of the expression of *fis1* transcripts using RNAscope (Supplementary Figure S2) showed consistency with RT-qPCR data, with increased expression detected in the photoreceptors and RPE at 8 dpf and 12 mpf.

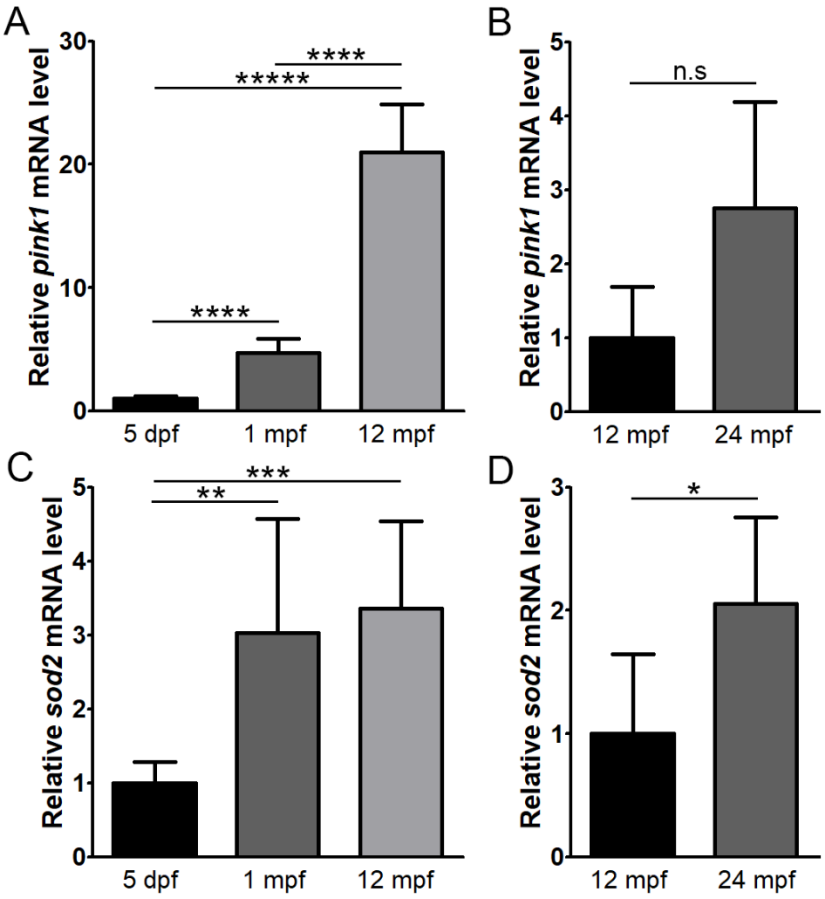

Figure 7. Expression levels of *pink1* and *sod2* with age in the zebrafish retina. RT-qPCR was performed to assess expression of *pink1* (**A**,**B**) and *sod2* (**C**,**D**) at 5 days post-fertilisation (dpf), 1 month post-fertilisation (mpf), 12 mpf and 24 mpf (n = 5). * $p < 0.05$; ** $p < 0.01$; *** $p < 0.001$; **** $p < 0.00001$; ***** $p < 0.0000001$; n.s, not significant.

Expression of the mitophagy marker, *pink1*, showed significant upregulation with age, with a 4.7 ± 1.16 fold and 21.0 ± 3.9 fold expression at 1 mpf and 12 mpf, respectively, relative to 5 dpf ($p < 0.0001$ and $p < 0.0000001$, n = 5) (Figure 7A). The increase in expression between 12 mpf and 24 mpf was not significant ($p = 0.09$) (Figure 7B). *sod2* expression showed a 3.0 ± 1.54 fold at 1 mpf compared to 5 dpf ($p < 0.01$, n = 5) and then maintained a similar level of expression of 12 mpf (Figure 7C). At 24 mpf, expression was increased by 2.1 ± 0.71 fold relative to 12 mpf ($p < 0.05$, n = 5) (Figure 7D).

4. Discussion

Mitochondria play an essential role in the homeostasis and function of the retina and are intrinsically linked to ageing and disease. In this study, we examined ultrastructural changes in mitochondrial morphology along with associated gene expression patterns to determine how these change in ageing zebrafish retina. This has provided new insights into species specific differences relating to how mitochondria adapt and mature from early development through to later stages of the lifecycle.

As zebrafish age, greater expression of both *opa1* and *fis1* was found within the retina, indicating increasing degrees of mitochondria remodelling with age. Higher relative expression levels of *fis1* were found, compared to *opa1,* with ageing, which favours mitochondria fission over fusion. This coincides with an increase in mitochondria number and reduction in their size with age, as measured within the RPE and rod and UV cone photoreceptors. The most noticeable difference in RPE mitochondria number and size occurred within 1 mpf. At 5 dpf, large mitochondria are present in the RPE that are most likely precursors to the smaller and more numerous mitochondria present at 8 dpf. This is likely driven by fission events and coincides with increased expression of *fis1* at 8 dpf that was not seen at 6 or 7 dpf. From 1 mpf through to 36 mpf, the mitochondria continue to reduce in size and increase in number but at a more gradual rate. As fission occurs, mitochondrial DNA is distributed across a larger number of mitochondria and previous studies have indicated this can lead to an increase in mitochondrial DNA replication [28]. This may explain the increasing expression levels with age of *polg2*, which encodes p55, an accessory subunit of polymerase gamma involved in mitochondrial DNA replication [29]. In studies examining the ageing human retina, changes in the size and number of mitochondria within the RPE have been assessed. Between ~40 to 90 years of age, mitochondria were found to reduce in size similarly to ageing zebrafish, but in contrast the number of mitochondria reduced with age [18,19].

Zebrafish at 5 dpf had mitochondria within the RPE, rod ISs and UV cone ISs that had a morphology distinct from that at later timepoints. Large mitochondria were present within the different cell types and in the rod and UV cone photoreceptors were bundled together in a spherical like arrangement, as previously reported [22]. At 8 dpf within the RPE, the mitochondria have an appearance in between the large ones seen at 5 dpf and the smaller mitochondria seen at 1 mpf. By 1 mpf, the rod and cone photoreceptor mitochondria no longer have a spherical arrangement and instead there is an ellipsoid-like configuration. Electron tomography (ET) provided higher resolution data in 3D in comparison to conventional TEM imaging. This allowed detailed assessment of the mitochondrial morphology within photoreceptor ISs at 5 dpf. The arrangement of the cristae in mitochondria in each cell type differed and may relate to the specialised function and environment of the cells. The rods have long sheet-like cristae with membranes that are closely opposed, whereas the UV cone mitochondrial cristae have a more tubular-like morphology that has greater spacing between membranes. Uniform spacing of the outer mitochondrial membranes was found in both rod and UV cone ISs and this likely results from tethering complexes that reside in between opposing mitochondrial membranes. These would act to hold the mitochondria together and keep them a specific distance apart similar to tethers found for contact sites between organelles such as the endoplasmic reticulum and lysosomes or mitochondria [30].

The term megamitochondria has been used to describe mitochondria that have diameters that exceed 2 μm. This includes the large mitochondria of the photoreceptor in some species of shrew as well as zebrafish (evident in all zebrafish ages examined in this study) [7,8,10]. Due to the large size of RPE mitochondria at 5 dpf, these too can be classified as megamitochondria. Previous work has shown the megamitochondria in zebrafish photoreceptors generate high levels of energy that are likely to be required to help fulfil the substantial energy demand of these cells [11]. Megamitochondria have also been reported to be an indicator of disease as they can occur in hepatic dysfunction [31]. Here we report the existence of physiological megamitochondria within the RPE cells for the first time. It is likely they have not been described previously due to being replaced after 5 dpf with smaller mitochondria. Further work is required to understand why these megamitochondria exist in the RPE, particularly to examine the mechanism that underlies the biogenesis of these organelles.

Changes in mitochondrial morphology with age within mature zebrafish retina could result from adaptations to compensate for oxidative stress as a result of continued light exposure and the mechanisms that underlie the visual cycle. Light exposure leads to

oxygen-related stress of retinal cells including the photoreceptors and RPE as shown with constant LED lighting studies using rats and cell culture models [14,32]. Phagocytosis of photoreceptor outer segments by the RPE exposes the cells to high levels of free radicals on a daily basis [13]. Oxidative damage has been shown to cause mitochondrial DNA modifications that can lead to mitophagy [32,33]. The expression levels of *pink1* and *sod2* were examined as indicators of mitochondrial stress and an oxidative environment. *pink1* encodes a mitophagy protein required in the selective degradation of damaged mitochondria and *sod2* has been implicated in cardioprotection during oxidative stress by converting superoxide into less damaging species [34,35]. *pink1* showed greatly increased expression at 12 mpf indicating continued stress and turnover of mitochondria within the retina that increases with time, whereas *sod2* had a less substantial increase but still indicated prolonged oxidative stress of the retina compared to the early timepoint at 5 dpf. These observations fit with cellular stress within the retina that increases with age. As individual mitochondria become less efficient due to increasing oxidants with age, upregulated fission could compensate by generating additional mitochondria to fulfil the energy demands.

Developing and mature mouse retinas were examined to determine if a similar morphological change in RPE and photoreceptor mitochondria were evident. Mice mainly have rod photoreceptors and by E14, mouse retinas do not have fully developed photoreceptor OSs. By P13, the mouse retina has a similar appearance to the 5 dpf zebrafish (the earliest point we examined) as the OSs has almost fully formed in both. When examining mouse retina at E14 and P13 and comparing to 6-month adult retina, there was no clear difference in morphology of the RPE mitochondria. In contrast to zebrafish, mouse photoreceptor ISs mitochondria appeared to increase in size between the earliest timepoint examined (E14) and adulthood (6 months). It is known that mitochondria within photoreceptor ISs change during retinal development, including repositioning of the mitochondria up to postnatal day 21 as shown previously [36]. Even so, they do not present the same packing of mitochondria as seen in developing zebrafish photoreceptor ISs. Mice IS mitochondria are orientated along the long axis of the IS with most running alongside and in contact with the plasma membrane [36]. In contrast, zebrafish IS are more densely packed with mitochondria that are positioned against the plasma membrane but also throughout the IS and their membranes are closely associated with each other. This dense packing of mitochondria throughout the IS of zebrafish appears to be more similar to human than mouse photoreceptors [37]. This could be due to humans and zebrafish being diurnal and may have a role in the recently discovered way that photoreceptor mitochondria act as microlenses to focus light through to the outer segment [38]. Further work is required to determine if the packing of mitochondria in the developing zebrafish photoreceptor ISs and fission into smaller mitochondria in these cells and RPE occurs in other species.

5. Conclusions

This work provides an overview of the changes in mitochondrial morphology and gene expression in developing and ageing zebrafish. The ability for mitochondria to adapt to their surroundings during ageing is essential for cellular health and function. Changes in the mitochondria detected in zebrafish in this study provide an excellent basis for future studies of retinal diseases that are linked to mitochondrial dysfunction.

Supplementary Materials: The following supporting information can be downloaded at: https://www.mdpi.com/article/10.3390/cells11223542/s1, Figure S1: Further examples of mitochondria within the RPE at 5 days post-fertilisation (dpf). Figure S2: Electron microscopy images of mitochondria within the inner segment of rod and UV cone photoreceptors at 5 days post-fertilisation (dpf). Figure S3: Expression levels of *mfn1* with age in the zebrafish retina. Figure S4: Expression of *fis1* (green) and *opa1* (red) mRNA in zebrafish photoreceptors and retinal pigment epithelium (RPE) at 5 days post-fertilisation (dpf), 8 dpf, 1 month post-fertilisation (mpf), and 12 mpf. Video S1: Tomogram showing rod photoreceptor inner segment of 5 pdf zebrafish. Video S2: Tomogram showing UV cone photoreceptor inner segment of 5 pdf zebrafish.

Author Contributions: Conceptualization, M.M.; investigation, T.B., M.T., C.W. and D.T.-W.; resources, C.E.F. and M.M.; data curation, T.B. and M.T.; writing—original draft preparation, T.B. and M.T.; writing—review and editing, T.B., M.T., C.E.F. and M.M.; funding acquisition, M.M. All authors have read and agreed to the published version of the manuscript.

Funding: This research was funded by Wellcome Trust, grant numbers 205174/Z/16/Z (M.M.) and 212216/Z/18/Z (C.E.F.), Sight Research UK and Moorfields Eye Charity (M.M.).

Institutional Review Board Statement: Zebrafish were maintained according to local UCL and UK Home Office regulations for the care and use of laboratory animals under the Animals Scientific Procedures Act, at the UCL Institute of Ophthalmology animal facility. UCL Animal Welfare and Ethical Review Body approved all procedures for experimental protocols, in addition to the UK Home Office (License no. PPL PC916FDE7). All approved standard protocols followed the guidelines of the Association for Research in Vision and Ophthalmology (ARVO) Statement for the Use of Animals in Ophthalmic and Vision Research Ethics [23]. Eyes acquired from mice killed by cervical dislocation was done in accordance with Home Office (United Kingdom) guidance rules under project license 70/8401. This adhered to the ARVO Statement for the Use of Animals in Ophthalmic and Vision Research.

Informed Consent Statement: Not applicable.

Data Availability Statement: Data is contained within the article or Supplementary Materials.

Conflicts of Interest: The authors declare no conflict of interest.

References

1. Lefevere, E.; Toft-Kehler, A.K.; Vohra, R.; Kolko, M.; Moons, L.; Van Hove, I. Mitochondrial Dysfunction Underlying Outer Retinal Diseases. *Mitochondrion* **2017**, *36*, 66–76. [CrossRef] [PubMed]
2. Eells, J.T. Mitochondrial Dysfunction in the Aging Retina. *Biology* **2019**, *8*, 31. [CrossRef] [PubMed]
3. Chan, D.C. Mitochondrial Dynamics and Its Involvement in Disease. *Annu. Rev. Pathol.* **2020**, *15*, 235–259. [CrossRef] [PubMed]
4. Yu-Wai-Man, P.; Newman, N.J. Inherited Eye-Related Disorders Due to Mitochondrial Dysfunction. *Hum. Mol. Genet.* **2017**, *26*, R12–R20. [CrossRef]
5. Medrano, C.J.; Fox, D.A. Oxygen Consumption in the Rat Outer and Inner Retina: Light- and Pharmacologically-Induced Inhibition. *Exp. Eye. Res.* **1995**, *61*, 273–284. [CrossRef]
6. Kam, J.H.; Jeffery, G. To Unite or Divide: Mitochondrial Dynamics in the Murine Outer Retina That Preceded Age Related Photoreceptor Loss. *Oncotarget* **2015**, *6*, 26690–26701. [CrossRef]
7. Lluch, S.; López-Fuster, M.J.; Ventura, J. Giant Mitochondria in the Retina Cone Inner Segments of Shrews of Genus Sorex (Insectivora, Soricidae). *Anat. Rec. A Discov. Mol. Cell. Evol. Biol.* **2003**, *272*, 484–490. [CrossRef]
8. Knabe, W.; Kuhn, H.J. Morphogenesis of Megamitochondria in the Retinal Cone Inner Segments of Tupaia Belangeri (Scandentia). *Cell Tissue Res.* **1996**, *285*, 1–9. [CrossRef]
9. Nag, T.C.; Wadhwa, S.; Chaudhury, S. The Occurrence of Cone Inclusions in the Ageing Human Retina and Their Possible Effect upon Vision: An Electron Microscope Study. *Brain Res. Bull.* **2006**, *71*, 224–232. [CrossRef]
10. Kim, J.; Lee, E.; Chang, B.S.; Oh, C.S.; Mun, G.-H.; Chung, Y.H.; Shin, D.H. The Presence of Megamitochondria in the Ellipsoid of Photoreceptor Inner Segment of the Zebrafish Retina. *Anat. Histol. Embryol.* **2005**, *34*, 339–342. [CrossRef]
11. Masuda, T.; Wada, Y.; Kawamura, S. ES1 Is a Mitochondrial Enlarging Factor Contributing to Form Mega-Mitochondria in Zebrafish Cones. *Sci. Rep.* **2016**, *6*, 22360. [CrossRef] [PubMed]
12. Jarrett, S.G.; Lin, H.; Godley, B.F.; Boulton, M.E. Mitochondrial DNA Damage and Its Potential Role in Retinal Degeneration. *Prog. Retin. Eye. Res.* **2008**, *27*, 596–607. [CrossRef]
13. Upadhyay, M.; Milliner, C.; Bell, B.A.; Bonilha, V.L. Oxidative Stress in the Retina and Retinal Pigment Epithelium (RPE): Role of Aging, and DJ-1. *Redox. Biol.* **2020**, *37*, 101623. [CrossRef] [PubMed]
14. Benedetto, M.M.; Contin, M.A. Oxidative Stress in Retinal Degeneration Promoted by Constant LED Light. *Front. Cell. Neurosci.* **2019**, *13*, 139. [CrossRef] [PubMed]
15. Toms, M.; Burgoyne, T.; Tracey-White, D.; Richardson, R.; Dubis, A.M.; Webster, A.R.; Futter, C.; Moosajee, M. Phagosomal and Mitochondrial Alterations in RPE May Contribute to KCNJ13 Retinopathy. *Sci. Rep.* **2019**, *9*, 3793. [CrossRef] [PubMed]
16. Formosa, L.E.; Ryan, M.T. Mitochondrial Fusion: Reaching the End of Mitofusin's Tether. *J. Cell. Biol.* **2016**, *215*, 597–598. [CrossRef]
17. Liu, Y.J.; McIntyre, R.L.; Janssens, G.E.; Houtkooper, R.H. Mitochondrial Fission and Fusion: A Dynamic Role in Aging and Potential Target for Age-Related Disease. *Mech. Ageing Dev.* **2020**, *186*, 111212. [CrossRef]
18. Bianchi, E.; Scarinci, F.; Ripandelli, G.; Feher, J.; Pacella, E.; Magliulo, G.; Gabrieli, C.B.; Plateroti, R.; Plateroti, P.; Mignini, F.; et al. Retinal Pigment Epithelium, Age-Related Macular Degeneration and Neurotrophic Keratouveitis. *Int. J. Mol. Med.* **2013**, *31*, 232–242. [CrossRef]

19. Feher, J.; Kovacs, I.; Artico, M.; Cavallotti, C.; Papale, A.; Balacco Gabrieli, C. Mitochondrial Alterations of Retinal Pigment Epithelium in Age-Related Macular Degeneration. *Neurobiol. Aging* **2006**, *27*, 983–993. [CrossRef]
20. Gouras, P.; Ivert, L.; Neuringer, M.; Nagasaki, T. Mitochondrial Elongation in the Macular RPE of Aging Monkeys, Evidence of Metabolic Stress. *Graefes. Arch. Clin. Exp. Ophthalmol.* **2016**, *254*, 1221–1227. [CrossRef]
21. Tarboush, R.; Chapman, G.B.; Connaughton, V.P. Ultrastructure of the Distal Retina of the Adult Zebrafish, Danio Rerio. *Tissue Cell* **2012**, *44*, 264–279. [CrossRef] [PubMed]
22. Tarboush, R.; Novales Flamarique, I.; Chapman, G.B.; Connaughton, V.P. Variability in Mitochondria of Zebrafish Photoreceptor Ellipsoids. *Vis. Neurosci.* **2014**, *31*, 11–23. [CrossRef] [PubMed]
23. Westerfield, M. *The Zebrafish Book: A Guide for the Laboratory Use of Zebrafish (Danio Rerio)*; University of Oregon Press: Eugene, OR, USA, 2020.
24. Crespo, C.; Knust, E. Characterisation of Maturation of Photoreceptor Cell Subtypes during Zebrafish Retinal Development. *Biol. Open* **2018**, *7*, bio036632. [CrossRef]
25. Heavner, W.; Pevny, L. Eye Development and Retinogenesis. *Cold Spring Harb Perspect. Biol.* **2012**, *4*, a008391. [CrossRef] [PubMed]
26. Richardson, R.; Tracey-White, D.; Webster, A.; Moosajee, M. The Zebrafish Eye—A Paradigm for Investigating Human Ocular Genetics. *Eye* **2017**, *31*, 68–86. [CrossRef]
27. Rochefort, N.L.; Garaschuk, O.; Milos, R.-I.; Narushima, M.; Marandi, N.; Pichler, B.; Kovalchuk, Y.; Konnerth, A. Sparsification of Neuronal Activity in the Visual Cortex at Eye-Opening. *Proc. Natl. Acad. Sci. USA* **2009**, *106*, 15049–15054. [CrossRef]
28. Chapman, J.; Ng, Y.S.; Nicholls, T.J. The Maintenance of Mitochondrial DNA Integrity and Dynamics by Mitochondrial Membranes. *Life* **2020**, *10*, 164. [CrossRef]
29. Longley, M.J.; Clark, S.; Yu Wai Man, C.; Hudson, G.; Durham, S.E.; Taylor, R.W.; Nightingale, S.; Turnbull, D.M.; Copeland, W.C.; Chinnery, P.F. Mutant POLG2 Disrupts DNA Polymerase Gamma Subunits and Causes Progressive External Ophthalmoplegia. *Am. J. Hum. Genet.* **2006**, *78*, 1026–1034. [CrossRef]
30. Picard, M.; McManus, M.J.; Csordás, G.; Várnai, P.; Dorn Ii, G.W.; Williams, D.; Hajnóczky, G.; Wallace, D.C. Trans-Mitochondrial Coordination of Cristae at Regulated Membrane Junctions. *Nat. Commun.* **2015**, *6*, 6259. [CrossRef]
31. Tandler, B.; Hoppel, C.L. Giant Mitochondria (Megamitochondria). In *Encyclopedia of Biological Chemistry*, 2nd ed.; Lennarz, W.J., Lane, M.D., Eds.; Academic Press: Waltham, MA, USA, 2013; pp. 375–376. ISBN 978-0-12-378631-9.
32. Godley, B.F.; Shamsi, F.A.; Liang, F.-Q.; Jarrett, S.G.; Davies, S.; Boulton, M. Blue Light Induces Mitochondrial DNA Damage and Free Radical Production in Epithelial Cells. *J. Biol. Chem.* **2005**, *280*, 21061–21066. [CrossRef]
33. Dan, X.; Babbar, M.; Moore, A.; Wechter, N.; Tian, J.; Mohanty, J.G.; Croteau, D.L.; Bohr, V.A. DNA Damage Invokes Mitophagy through a Pathway Involving Spata18. *Nucleic Acids Res.* **2020**, *48*, 6611–6623. [CrossRef] [PubMed]
34. Jin, S.M.; Youle, R.J. PINK1- and Parkin-Mediated Mitophagy at a Glance. *J. Cell. Sci.* **2012**, *125*, 795–799. [CrossRef] [PubMed]
35. Flynn, J.M.; Melov, S. SOD2 in Mitochondrial Dysfunction and Neurodegeneration. *Free Radic. Biol. Med.* **2013**, *62*, 4–12. [CrossRef]
36. Meschede, I.P.; Ovenden, N.C.; Seabra, M.C.; Futter, C.E.; Votruba, M.; Cheetham, M.E.; Burgoyne, T. Symmetric Arrangement of Mitochondria:Plasma Membrane Contacts between Adjacent Photoreceptor Cells Regulated by Opa1. *Proc. Natl. Acad. Sci. USA* **2020**, *117*, 15684–15693. [CrossRef]
37. Nag, T.C.; Wadhwa, S. Immunolocalisation Pattern of Complex I–V in Ageing Human Retina: Correlation with Mitochondrial Ultrastructure. *Mitochondrion* **2016**, *31*, 20–32. [CrossRef] [PubMed]
38. Ball, J.M.; Chen, S.; Li, W. Mitochondria in Cone Photoreceptors Act as Microlenses to Enhance Photon Delivery and Confer Directional Sensitivity to Light. *Sci. Adv.* **2022**, *8*, eabn2070. [CrossRef] [PubMed]